

# Synthesis and characterization of a novel magnetic nano-palladium Schiff base complex: application in cross-coupling reactions

Millad Aghayee<sup>a</sup>, Mohammad Ali Zolfigol<sup>b\*</sup>, Hassan Keypour<sup>a</sup>, Meysam Yarie<sup>b</sup> and Leila Mohammadi<sup>b</sup>



A novel and task-specific nano-magnetic Schiff base ligand with phosphate spacer using 2-aminoethyl dihydrogen phosphate instead of usual coating agents, i.e. tetraethoxysilane and 3-aminopropyltriethoxysilane, for coating of nano-magnetic Fe<sub>3</sub>O<sub>4</sub> is introduced. The nano-magnetic Schiff base ligand with phosphate spacer as a novel catalyst was synthesized and fully characterized using infrared spectroscopy, X-ray diffraction, scanning and transmission electron microscopies, thermogravimetry, derivative thermogravimetry, vibrating sample magnetometry, atomic force microscopy, X-ray photoelectron spectroscopy and energy-dispersive X-ray spectroscopy. The resulting task-specific nano-magnetic Schiff base ligand with phosphate spacer was successfully employed as a magnetite Pd nanoparticle-supported catalyst for Sonogashira and Mizoroki–Heck C–C coupling reactions. To the best of our knowledge, this is the first report of the synthesis and applications of magnetic nanoparticles of Fe<sub>3</sub>O<sub>4</sub>@O<sub>2</sub>PO<sub>2</sub>(CH<sub>2</sub>)<sub>2</sub>NH<sub>2</sub> as a suitable spacer for the preparation of a designable Schiff base ligand and its corresponding Pd complex. So the present work can open up a new and promising insight in the course of rational design, synthesis and applications of various task-specific magnetic nanoparticle complexes. Copyright © 2016 John Wiley & Sons, Ltd.

Additional supporting information may be found in the online version of this article at the publisher's web site.

**Keywords:** task-specific nano-magnetic Schiff base ligand; 2-aminoethyl dihydrogen phosphate; Sonogashira and Mizoroki–Heck C–C coupling reactions; magnetite Pd nanoparticle-supported catalyst

## Introduction

Nowadays, novel approaches focus on sustainable development of highly selective nanostructured catalysts by designing and applying suitable catalytic species and central cores.<sup>[1]</sup> There are extensive reports wherein silica derivatives have been employed as coating agents for the synthesis of nano-magnetic catalysts, possessing several outstanding features such as high activity and selectivity, excellent stability, efficient recovery and recyclability.<sup>2</sup>

Therefore, knowledge-based design, synthesis and applications of powerful, recyclable and reusable nano-magnetic catalysts are in demand. Literature surveys show that heterogeneous catalysts in chemical processes have attracted a great deal of attention due to their merits such as easy separation from the reaction mixture and good reusability compared to homogeneous catalytic systems. One important issue that has to be considered in terms of using heterogeneous catalytic systems compared with homogeneous ones is the low activity and selectivity because of the low surface area. Also, in the case of immobilization of a catalytically active species on a suitable support, this problem is more serious. In this case, the active sites in a supported system, due to the steric hindrance of the bulky support, are not as approachable as those in a homogeneous equivalent. Combination of nanotechnology and heterogeneous catalytic systems can overcome the drawbacks connected with bulky supports by miniaturizing the size of the support. This approach leads to an increase of the ratio of surface to volume and consequently can multiply the interactions of surface and reactants. Notwithstanding that, nano-chemistry technology can draw

near homogeneous and heterogeneous catalytic systems from activity and selectivity outlooks, but the easy separation and recovery of the catalyst are still major restrictions for nanomaterials due to their very small dimensions. The knowledge-based development of the science of catalysts leads chemists to create and use magnetic nanoparticles as excellent alternatives which can be easily separated from the reaction mixture by applying a simple external magnet. Also, the magnetization of common nano-solid supports is an excellent method for overcoming the difficulty in the separation of catalysts from reaction mixtures. The combination of heterogeneous properties, nano-chemistry technology and magnetic solid supports can create a new class of heterogeneous recoverable and reusable catalytic systems that have the benefits of homogeneous catalysts, such as high activity and selectivity.<sup>[2–4]</sup>

The Sonogashira cross-coupling reaction which constructs C(sp<sup>2</sup>)–C(sp) bonds leading to arylalkynes and conjugated enynes using homogeneous and heterogeneous palladium catalysts in the presence or absence of Cu(I) as a co-catalyst<sup>[5–9]</sup> is a straightforward route to pharmaceutical and biologically active molecules such as tazarotene (**1**)<sup>[10]</sup> for the treatment of psoriasis and acne and altincline (**2**)<sup>[11]</sup> for the therapy of Parkinson's disease,

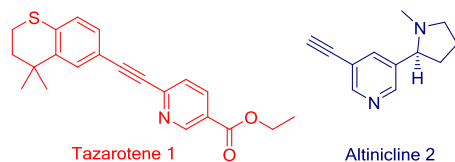
\* Correspondence to: Mohammad Ali Zolfigol, Faculty of Chemistry, Bu-Ali Sina University, Hamedan, 6517838683, Iran. E-mail: zolfi@basu.ac.ir; mzolfigol@yahoo.com

<sup>a</sup> Faculty of Chemistry, Bu-Ali Sina University, Hamedan 65174, Iran

<sup>b</sup> Faculty of Chemistry, Bu-Ali Sina University, Hamedan 6517838683, Iran

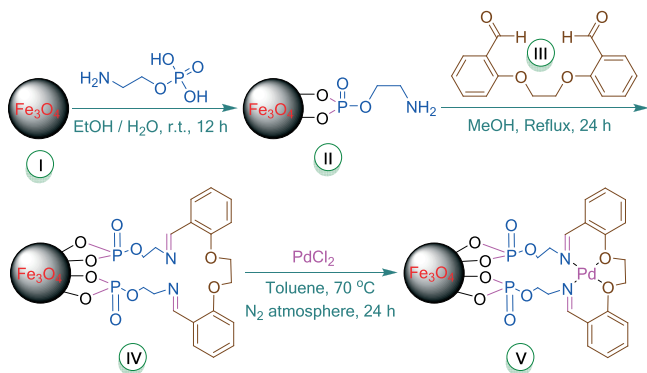
Alzheimer's disease, Tourette syndrome, schizophrenia and attention deficit hyperactivity disorder.

The Mizoroki–Heck reaction is a very powerful and effective procedure for the preparation of substituted alkenes through the reaction of unsaturated halides, triflates and diazoniums with an alkene in the presence of a suitable base and palladium catalyst or palladium nanomaterial-based catalyst.<sup>[12–14]</sup> Also, the resulting products from the Heck reaction have shown a wide variety of applications in the pharmaceutical industry.<sup>[15]</sup>



2-Aminoethyl dihydrogen phosphate, aminoethyl phosphate or phosphorylethanolamine (with two  $pK_a$  values of 5.61 and 10.39) is an ethanolamine derivative that is used to build up sphingomyelins (sphingomyelin is a type of sphingolipid that can be found in animal cell membranes, particularly in the membranous myelin sheath that surrounds some nerve cell axons). Also, it has been reported that synthetic phosphorylethanolamine can act as a treatment for Ehrlich ascites tumour cells in cancer therapy.<sup>[16,17]</sup> Very recently, Zarghani and Akhlaghnia reported Cu(II) immobilized on aminated ferrite nanoparticles using 2-aminoethyl dihydrogen phosphate ( $Fe_3O_4@AEPH_2-Cu^{II}$ ) for conversion of aldoximes to nitriles.<sup>[18]</sup> They have also reported a sulfonated nanohydroxyapatite functionalized with 2-aminoethyl dihydrogen phosphate ( $HAP@AEPH_2-SO_3H$ ) as a new green, recyclable, solid acid catalyst for the one-pot synthesis of 4,4'-(aryl methylene)bis(3-methyl-1H-pyrazol-5-ol)s.<sup>[19]</sup> Also, Yilmaz and co-workers reported the synthesis of novel calixarene-functionalized iron oxide magnetite nanoparticles and investigated the extraction abilities of these extractants for the removal of dichromate/arsenate ions from water.<sup>[20]</sup>

As is known, 2-aminoethyl dihydrogen phosphate has a dual role: it can act as both spacer and coating agent in the synthetic processes of our designed magnetic nanocatalysts. Thus, we do not need any use of silica coating agent for the covering of central magnetic  $Fe_3O_4$  nanoparticles. In continuation of our knowledge-based development of task-specific nano-magnetic catalysts,<sup>[21]</sup> herein, we report the preparation of a novel task-specific nano-magnetic Schiff base ligand with phosphate spacer and the applications of its resulting Pd nano-magnetic heterogeneous catalyst in the Sonogashira and Mizoroki–Heck reactions (Schemes 1 and 2).



**Scheme 1.** Preparation of novel task-specific nano-magnetic Schiff base ligand with phosphate spacer and its Pd nano-magnetic heterogeneous catalyst.



**Scheme 2.** Applicability of the novel Pd-based catalyst in C–C coupling reactions.

## Results and discussion

The structure of the nano-magnetic Schiff base ligand with phosphate spacer as a novel catalyst was fully investigated using various methods such as: infrared (IR) spectroscopy, X-ray diffraction (XRD), scanning electron microscopy (SEM), transmission electron microscopy (TEM), thermogravimetry (TG), vibrating sample magnetometry (VSM), atomic force microscopy (AFM) and energy-dispersive X-ray (EDX) analysis.

The broad absorption band in the region of about  $3000\text{--}3600\text{ cm}^{-1}$  in the IR spectra can be attributed to the overlapping of uncoated O–H and  $NH_2$  group stretching modes of compound II, and also the  $P=O$  stretching mode is verified by observation of a peak at  $1142\text{ cm}^{-1}$  (Fig. 1(b)). The reaction of compound II and dialdehyde

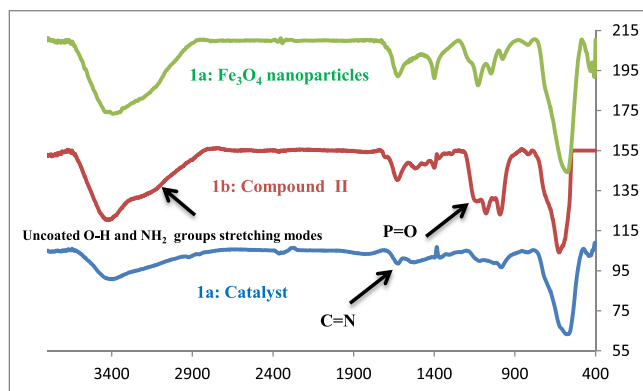


**Figure 1.** IR spectrum of the catalyst (c) in comparison with the IR spectra of compound II (b) and  $Fe_3O_4$  nanoparticles (a).

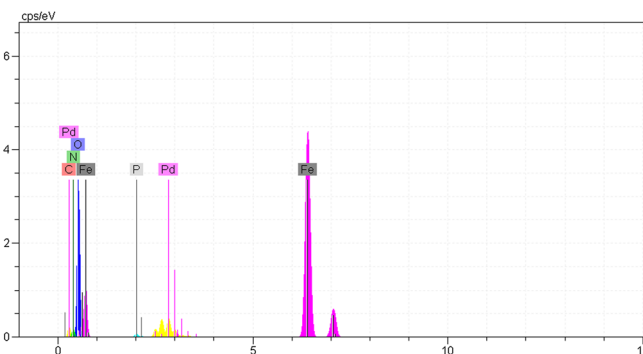


**Figure 2.** EDX analysis of the catalyst.

III and the formation of the catalyst are confirmed by the C=N band at  $1625\text{ cm}^{-1}$  in the IR spectrum of catalyst V (Fig. 1(c)).

The results of EDX spectroscopy confirm all the expected elements, namely carbon, nitrogen, oxygen, palladium, iron and phosphorus, as shown in Fig. 2. Moreover, the SEM-coupled EDX data for the new catalyst imply that it consists of C (0.04), N (3.25), Fe (65.60), O (24.17), Pd (6.59) and P (0.34).

Using VSM analysis, the magnetic behaviour of the novel nanocatalyst in comparison with  $\text{Fe}_3\text{O}_4$  nanoparticles was studied, as depicted in Fig. 3. According to the resulting magnetization curves, the saturation of the prepared catalyst reduces to  $64\text{ emu g}^{-1}$  from  $70\text{ emu g}^{-1}$ . This reduction in saturation arises from the surface coating of the  $\text{Fe}_3\text{O}_4$  nanoparticles in the synthetic pathway of the novel catalyst. It is worth mentioning that due to the direct connection of the Pd complex to the surface of the  $\text{Fe}_3\text{O}_4$  nanoparticles, the magnetic property of the new catalyst not very much reduced in comparison with other core-shell catalysts,<sup>[2–4]</sup> and this merit guarantees very facile and efficient separation of the catalyst from the reaction mixture due to the very good magnetic property.

TEM images of the new catalyst were recorded and are shown in Fig. 4. According to the TEM images, the sizes of the catalyst particles are less than 50 nm.

In addition to the TEM images (Fig. 4), in attempting to confirm of the size and morphology of the prepared catalyst, SEM images were recorded and are shown in Fig. 5. It can be inferred from the SEM images that the size of the catalyst particles is in the nanometre range in good accordance with the TEM images.

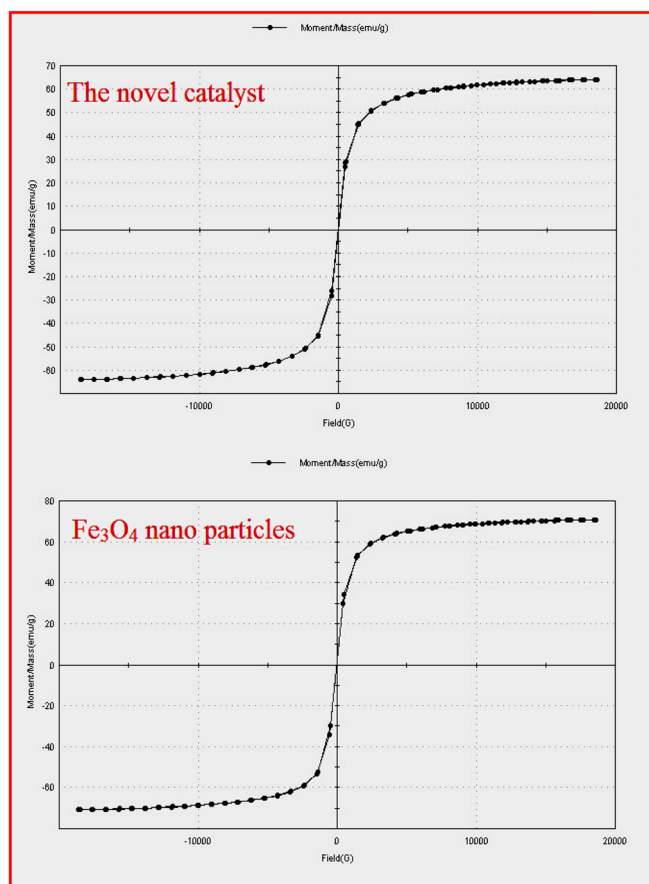


Figure 3. VSM analysis of novel catalyst and  $\text{Fe}_3\text{O}_4$  nanoparticles.

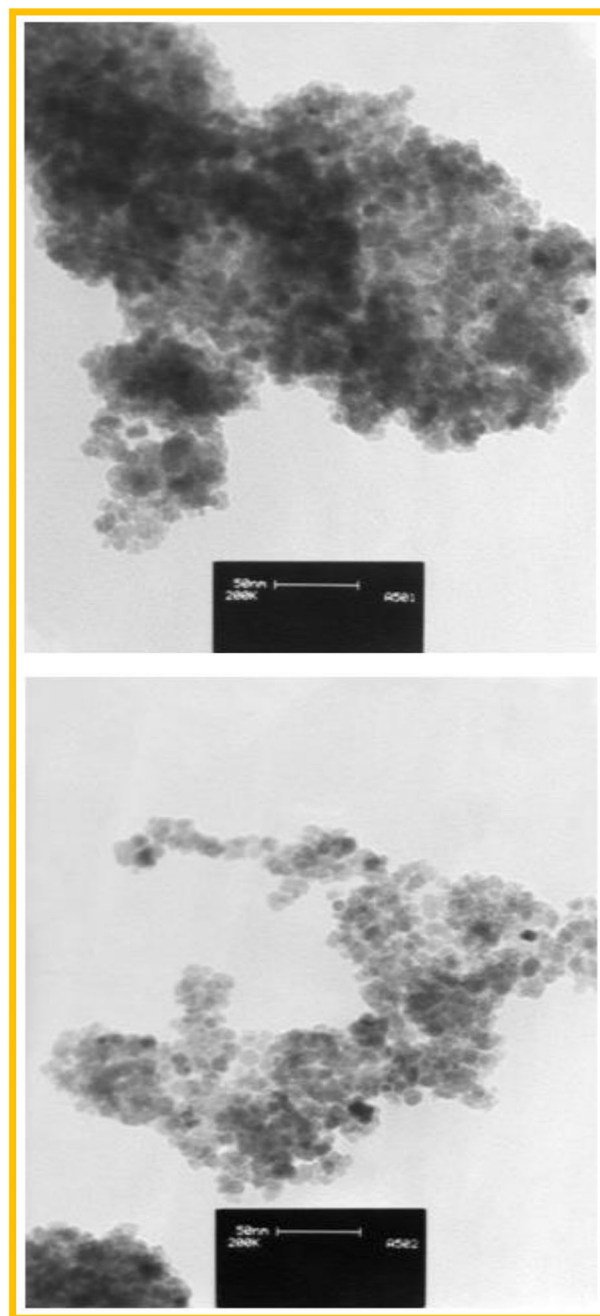


Figure 4. TEM images of the new catalyst.

The XRD pattern of the synthesized catalyst in comparison with those of  $\text{Fe}_3\text{O}_4$  nanoparticles and compound II was investigated as depicted in Fig. 6. It can be concluded from the XRD patterns that the addition of each layer onto the surface of the  $\text{Fe}_3\text{O}_4$  nanoparticles changes the corresponding XRD pattern compared with previous stage, being an indication of the preparation of the novel catalyst. The XRD pattern of the novel catalyst shows that it has a crystalline nature with diffraction lines at  $2\theta \approx 9.10^\circ, 16.70^\circ, 22.20^\circ, 22.80^\circ, 24.90^\circ, 30.70^\circ, 35.50^\circ, 36.00^\circ, 53.50^\circ, 57.30^\circ$  and  $62.90^\circ$ . In addition, the XRD data, including  $2\theta$  value, peak width, size of particles and interplanar distance, were extracted and are summarized in Table 1. It can be inferred from the extracted XRD data, based on the Scherrer equation  $D = K\lambda/(\beta \cos \theta)$ , where  $\lambda$  is the X-ray wavelength,  $K$  the Scherrer constant,  $\beta$  the peak width of half maximum

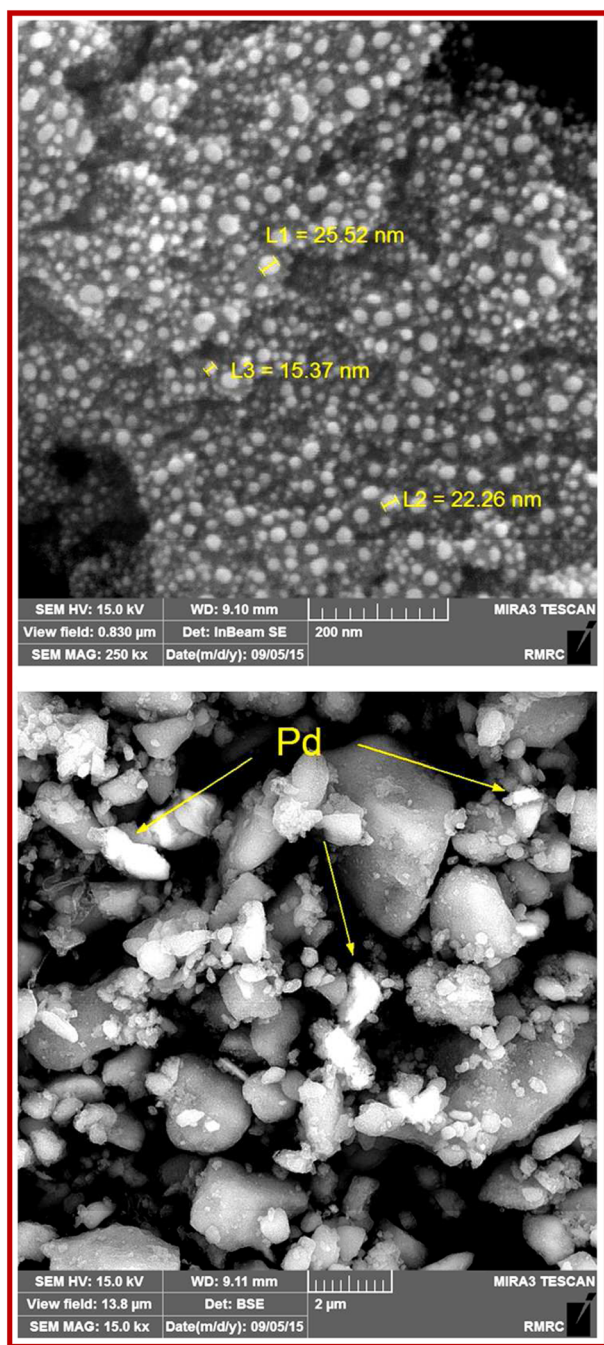


Figure 5. SEM images of the prepared catalyst.

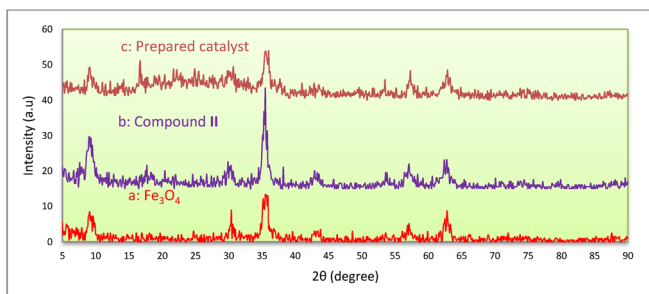


Figure 6. XRD pattern of synthesized catalyst in comparison with the patterns of  $\text{Fe}_3\text{O}_4$  nanoparticles and compound II.

Entry	$2\theta$ (°)	Peak width (FWHM) (°)	Size (nm)	Interplaner distance (nm)
1	9.10	0.50	15.94	0.158656
2	16.70	0.25	32.12	0.530233
3	22.20	0.34	23.87	0.799912
4	22.80	0.24	33.77	0.015219
5	24.90	0.36	22.60	0.357164
6	30.70	0.47	17.53	0.290879
7	35.60	0.30	27.81	0.251885
8	36.00	0.34	24.57	0.249178
9	53.50	0.16	55.61	0.171073
10	57.30	0.31	29.20	0.087742
11	62.90	0.33	28.22	0.147579

and  $\theta$  the Bragg diffraction angle, that the particle size of the catalyst is in the nanometre range of about 15.94–55.61 nm. It is noteworthy that the resulting data from the XRD pattern are in good agreement with the results from TEM and SEM images (Figs. 4 and 5).

Also, for the investigation of the surface topography and analysis of the surface at a high resolution of the novel Pd-based catalyst, a three-dimensional AFM image was obtained, as portrayed in Fig. 7. The three-dimensional  $5\ \mu\text{m} \times 5\ \mu\text{m}$  skeleton shows that the prepared nanocatalyst has a disturbed surface structure.

In order to determine the oxidation state of Pd in the complex, X-ray photoelectron spectroscopy (XPS) was conducted and the results are portrayed in Fig. 8. The binding energy pattern reveals

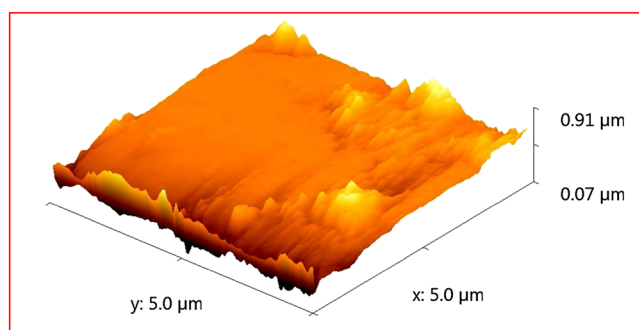


Figure 7. Three-dimensional AFM image of the surface of the Pd-based catalyst.

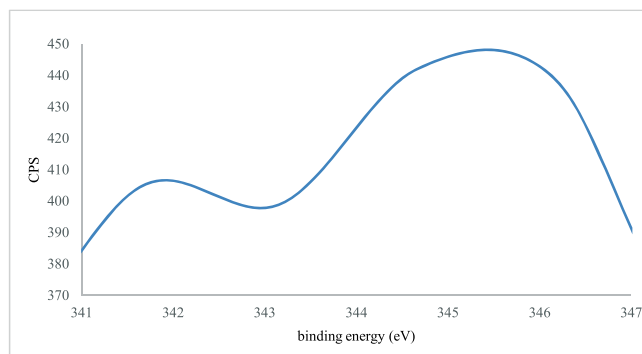


Figure 8. XPS spectra of the catalyst: Pd(0).

two peaks at 341.9 eV ( $3d_{5/2}$ ) and 345.4 eV ( $3d_{3/2}$ ) which can be attributed to the Pd(0) oxidation state.

After the structural verification of the prepared catalyst with the aforementioned techniques, the applicability of the catalyst was investigated in the Sonogashira and Mizoroki–Heck reactions (Scheme 2). In the first place, the reaction of phenylacetylene and bromobenzene was chosen as a test reaction. In order to determine the best experimental conditions for the Sonogashira reaction, various solvents, bases and loads of novel catalyst were checked and the resulting data are summarized in Table 2. It can be deduced from Table 2 that the optimized conditions for the Sonogashira reaction are when the reaction is performed using water as a green solvent,  $K_2CO_3$  as a base and utilizing a catalytic amount of prepared catalyst (Table 2, entry 2).

To investigate the generality and the versatility of the determined optimized reaction conditions, according to Table 2 for the Sonogashira cross-coupling reaction, the extent of the reaction was widened to other aryl halides as summarized in Table 3. The resulting data show that the reported method is applicable to other substrates and substituents with good to high yields being achieved in comparatively short reaction times.

In another experiment, the applicability of the prepared novel catalyst was probed in the Mizoroki–Heck reaction. In order to achieve the best experimental conditions for the reaction, the reaction between bromobenzene and styrene was chosen as a test reaction and the effect of various solvents, bases and loads of new catalyst was scrutinized. According to the obtained data as summarized in Table 4, the optimized conditions for the Mizoroki–Heck reaction in these surveys are when the reaction is carried out in acetonitrile as a solvent with  $K_2CO_3$  as base in the presence of the magnetically separable novel Pd-based catalyst (Table 4, entry 3).

In the case of the Mizoroki–Heck reaction, similar to the Sonogashira reaction, the versatility and the generality of the optimized conditions were checked for the reaction of various aryl

**Table 3.** Applicability of novel catalyst for a range of substrates in Sonogashira reaction

Entry	Aryl halide	Alkyne	Product	Time (min)	Yield (%) <sup>a</sup>
1	1-Bromobenzene	Phenylacetylene	<b>2a</b>	40	92
2	1-Iodobenzene	Phenylacetylene	<b>2a</b>	40	95
3	1-Bromo-4-nitrobenzene	Phenylacetylene	<b>2b</b>	42	88
4	2-Bromonaphthalene	Phenylacetylene	<b>2c</b>	54	83
5 <sup>b</sup>	1,4-Dibromobenzene	Phenylacetylene	<b>2d</b>	90	45
6	1,4-Dibromobenzene	Phenylacetylene	<b>2e</b>	80	40
7	1-Bromobenzene	1-Heptyne	<b>2f</b>	90	88
8	1-Iodobenzene	1-Heptyne	<b>2f</b>	85	91

<sup>a</sup>Isolated yields.

<sup>b</sup>Reaction performed with two equivalents of phenylacetylene in the presence of 10 mg of catalyst.

halides with styrene. The desired products are obtained in good to high yields in appropriate reaction times as summarized in Table 5.

Also, the possibility of recycling the prepared catalyst was explored for both types of cross-coupling reactions for nine runs. After the completion of the each run the catalyst was separated from the reaction mixture by applying a simple magnet and washed repeatedly with EtOH and recovered. In the case of the Sonogashira reaction, the re-use of the catalyst was examined for the reaction between phenylacetylene and bromobenzene under the optimized conditions in 40 min. In the case of the Mizoroki–Heck reaction, the reaction between styrene and bromobenzene was chosen as a model for the recycling test under the optimized conditions in

**Table 2.** Optimization of reaction conditions for Sonogashira reaction<sup>a</sup>

Entry	Catalyst amount (mg)	Base	Solvent <sup>b</sup>	Reaction time (min)	Yield (%) <sup>c</sup>
1	5	$K_2CO_3$	DMF	58	80
2	<b>5</b>	<b><math>K_2CO_3</math></b>	<b><math>H_2O</math></b>	<b>40</b>	<b>92</b>
3	5	$K_2CO_3$	$CH_3CN$	45	88
4	5	$K_2CO_3$	EtOH	48	85
5	5	$K_2CO_3$	MeOH	48	83
6	5	$K_2CO_3$	$CH_2Cl_2$	50	82
7	5	$Na_2CO_3$	$H_2O$	45	88
8	5	NaOH	$H_2O$	52	82
9	5	$Et_3N$	$H_2O$	60	78
10	5	$NH_3$	$H_2O$	60	70
11	5	DABCO	$H_2O$	60	68
12	3	$K_2CO_3$	$H_2O$	47	85
13	7	$K_2CO_3$	$H_2O$	40	92
14	10	$K_2CO_3$	$H_2O$	40	93

<sup>a</sup>Reaction conditions: phenylacetylene (1 mmol) and bromobenzene (1 mmol).

<sup>b</sup>Reflux.

<sup>c</sup>Isolated yield.

**Table 4.** Optimization of reaction conditions for Mizoroki–Heck reaction<sup>a</sup>

Entry	Catalyst amount (mg)	Base	Solvent <sup>b</sup>	Reaction time (h)	Yield (%) <sup>c</sup>
1	5	$K_2CO_3$	DMF	3	88
2	5	$K_2CO_3$	$H_2O$	3	85
3	<b>5</b>	<b><math>K_2CO_3</math></b>	<b><math>CH_3CN</math></b>	<b>3</b>	<b>92</b>
4	5	$K_2CO_3$	EtOH	3	80
5	5	$K_2CO_3$	MeOH	3	82
6	5	$K_2CO_3$	$CH_2Cl_2$	3	78
7	5	$Na_2CO_3$	$CH_3CN$	3	89
8	5	NaOH	$CH_3CN$	3	78
9	5	$Et_3N$	$CH_3CN$	3	75
10	5	$NH_3$	$CH_3CN$	3	65
11	5	DABCO	$CH_3CN$	3	60
12	3	$K_2CO_3$	$CH_3CN$	3	85
13	7	$K_2CO_3$	$CH_3CN$	3	92
14	10	$K_2CO_3$	$CH_3CN$	2.5	93

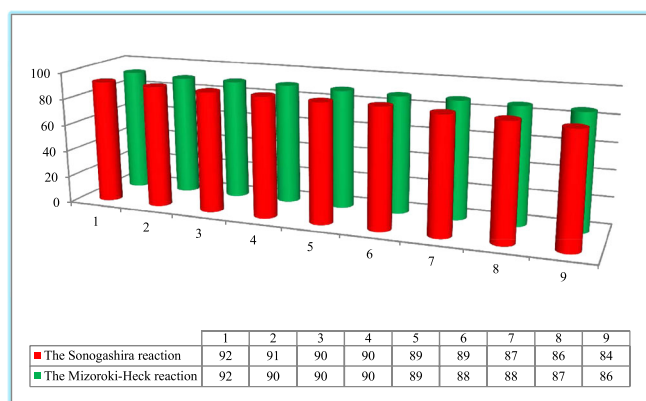
<sup>a</sup>Reaction conditions: styrene (1 mmol) and bromobenzene (1 mmol).

<sup>b</sup>Reflux.

<sup>c</sup>Isolated yield.

**Table 5.** Versatility of the new catalyst in Mizoroki–Heck reaction

Entry	Aryl Halide	Product	Reaction time (h)	Yield (%) <sup>a</sup>
1	1-Bromobenzene	<b>3a</b>	3	92
2	1-Iodobenzene	<b>3a</b>	2	95
3	1-Bromo-4-nitrobenzene	<b>3b</b>	3	90
4	1-Bromo-4-methylbenzene	<b>3c</b>	3	88
5	1-Bromo-4-methoxybenzene	<b>3d</b>	2	91
6	2-Bromonaphthalene	<b>3e</b>	20	86
7	1,4-Dibromobenzene	<b>3f</b>	4	45
8 <sup>b</sup>	1,4-Dibromobenzene	<b>3g</b>	4	55

<sup>a</sup>Isolated yields.<sup>b</sup>Reaction performed with two equivalents of styrene in the presence of 10 mg of catalyst.**Figure 9.** Recyclability of the prepared catalyst in both cases of cross-coupling reactions.

3 h. The data obtained are depicted in Fig. 9. Regardless of the type of coupling, the results indicate that the catalyst can be utilized several times (9 runs) without any significant loss of its initial catalytic activity which can be ascribed to the high stability of the prepared catalyst.

## Conclusions

In summary, we have developed a novel task-specific nano-magnetic Schiff base ligand with phosphate spacer using 2-aminoethyl dihydrogen phosphate for coating of magnetic Fe<sub>3</sub>O<sub>4</sub> nanoparticles. The structure of the resulting Pd-based nano-magnetic catalyst was fully confirmed using IR spectroscopy, XRD, SEM, TEM, TG, VSM, AFM, XPS and EDX analysis. The prepared task-specific nano-magnetic Schiff base ligand with phosphate spacer was successfully used as a magnetite Pd nanoparticle-supported catalyst for the Sonogashira and Mizoroki–Heck C–C coupling reactions. To the best of our knowledge, this is the first report of the synthesis and applications of magnetic nanoparticles of Fe<sub>3</sub>O<sub>4</sub>@O<sub>2</sub>PO<sub>2</sub>(CH<sub>2</sub>)<sub>2</sub>NH<sub>2</sub> as a suitable spacer for the preparation of designable Schiff base ligand and its corresponding Pd complex. So the present work can open up a new and promising insight in the course of rational design, synthesis and applications of various task-specific magnetic nanoparticle complexes.

## Experimental

### General

All chemicals were purchased from Fluka and Merck. The known products were identified by comparison of their physical properties and spectral data with those reported for authentic samples in the literature. Reaction progress and purity determination of the compounds were checked by TLC using silica gel SIL G/UV 254 plates. <sup>1</sup>H NMR and <sup>13</sup>C NMR spectra were recorded with a Bruker spectrometer. Melting points were recorded with a Buchi B-545 apparatus in open capillary tubes.

### Preparation of novel Pd-based catalyst

Initially, Fe<sub>3</sub>O<sub>4</sub> nanoparticles (**I**) were synthesized according to procedures reported in the literature.<sup>[21,22]</sup> In the second step, 1 g of **I** was added to 50 ml of a mixture of ethanol and deionized water. To the resulting mixture was added 2-aminoethyl dihydrogen phosphate (12 mmol, 1.69 g) dissolved in 20 ml of deionized water. The solution was stirred for 12 h at room temperature. Then, the resulting 2-aminoethyl dihydrogen phosphate-functionalized Fe<sub>3</sub>O<sub>4</sub> nanoparticles (**II**) were washed repeatedly with ethanol and deionized water and collected with a magnet and air-dried. To a mixture of **II** in 20 ml of methanol was added dialdehyde **III** (6 mmol, 1.62 g) followed by refluxing for 24 h. In the last step, the synthesized nanoparticles (**IV**) were added to a mixture of PdCl<sub>2</sub> dispersed in toluene as solvent and stirred vigorously for 24 h under nitrogen atmosphere at 70 °C. Finally, the resulting nano-magnetic Schiff base Pd complex catalyst with 2-aminoethyl phosphate spacers (**V**) was washed with ethanol and collected with an external magnet and air-dried (Scheme 1).

### General procedure for sonogashira reaction

To a round-bottom flask containing aryl halide (1 mmol) and phenylacetylene or 1-heptyne (1 mmol) were added K<sub>2</sub>CO<sub>3</sub> (1.5 mmol, 0.207 g) as a base, 5 ml of water as a solvent and 5 mg (0.002 mmol of Pd) of catalyst **V**. The resulting mixture was stirred vigorously at 90 °C for appropriate times as given in Table 2. After the completion of the reactions as monitored by TLC using *n*-hexane as eluent, the reaction mixture was quenched to ambient temperature. Then, 25 ml of Et<sub>2</sub>O was added to the solution and the organic layer was separated using a decanter and dried with Na<sub>2</sub>SO<sub>4</sub>. Finally, the crude products were purified with preparative TLC in high to excellent yields as summarized in Table 2. The prepared catalyst was separated by applying an external magnet and washed repeatedly with EtOH and recovered for the next run.

### General procedure for Mizoroki–Heck reaction

To a mixture of aryl halide (1 mmol) and styrene (1 mmol, 0.104 g) were added K<sub>2</sub>CO<sub>3</sub> (1.5 mmol, 0.207 g) as a base and 5 ml of CH<sub>3</sub>CN as a solvent in a round-bottom flask, to which was added 5 mg of Pd-based catalyst (0.002 mmol of Pd). The resulting mixture was refluxed for appropriate times as given in Table 4. When the reaction was completed, as monitored by TLC, the mixture was quenched to ambient temperature and 25 ml of *n*-hexane was added to the solution. The organic layer was separated and dried with Na<sub>2</sub>SO<sub>4</sub>. After evaporation of the solvent, the pure product was obtained in high to excellent yields. The catalyst was separated by applying an external magnet and washed repeatedly with EtOH and recovered for the next run.

## Acknowledgements

We thank Bu-Ali Sina University and Iran National Science Foundation (INSF) for financial support (Grant of Allameh Tabataba'i's Award) of our research group.

## References

- [1] R. K. Sharma, S. Sharma, S. Dutta, R. Zboril, M. B. Gawande, *Green Chem.* **2015**, *17*, 3207.
- [2] a) S. Rostamnia, E. Doustkhaha, *J. Mol. Catal. A* **2016**, *411*, 317; b) S. Rostamnia, E. Doustkhaha, *Synlett* **2015**, *26*, 1345.
- [3] B. Karimi, F. Mansouri, H. M. Mirzaei, *ChemCatChem* **2015**, *7*, 1736.
- [4] a) T. Cheng, D. Zhang, H. Li, G. Liu, *Green Chem.* **2014**, *16*, 3401; b) M. B. Gawande, R. Luque, R. Zboril, *ChemCatChem* **2014**, *6*, 3312; c) D. Zhang, C. Zhou, Z. Sun, L. Wu, C. Tunga, T. Zhang, *Nanoscale* **2012**, *4*, 6244.
- [5] a) K. Sonogashira, Y. Tohda, N. Hagihara, *Tetrahedron Lett.* **1975**, *16*, 4467; b) H. A. Dieck, F. R. Heck, *J. Organometal. Chem.* **1975**, *93*, 259; c) L. Cassar, *J. Organometal. Chem.* **1975**, *93*, 253.
- [6] a) M. Kotori, T. Takahashi, in *Handbook of Organopalladium Chemistry for Organic Synthesis* (Ed: E.-I. Negishi), John Wiley, New York, **2003**, p. 973; b) P. Siemsen, R. C. Livingston, F. Diederich, *Angew. Chem. Int. Ed.* **2000**, *39*, 2632.
- [7] a) D. Gelman, S. L. Buchwald, *Angew. Chem. Int. Ed.* **2003**, *42*, 5993; b) J. Liu, J. Chen, C. Xia, *J. Catal.* **2008**, *253*, 50; c) A. Corma, H. García, A. Primo, *J. Catal.* **2006**, *241*, 123; d) A. Corma, H. García, A. Leyva, *J. Catal.* **2006**, *240*, 87.
- [8] a) H. Huang, H. Liu, H. Jiang, K. Chen, *J. Org. Chem.* **2008**, *73*, 6037; b) Y. Liang, Y. X. Xie, J. H. Li, *J. Org. Chem.* **2006**, *71*, 379.
- [9] a) M. Pagliaro, V. Pandarus, R. Ciriminna, F. Beland, P. D. Cara, *ChemCatChem* **2012**, *4*, 432; b) M. Schilz, H. Plenio, *J. Org. Chem.* **2012**, *77*, 2798; c) R. Chinchilla, C. Najera, *Chem. Soc. Rev.* **2011**, *40*, 5084; d) R. Chinchilla, C. Najera, *Chem. Rev.* **2007**, *107*, 874.
- [10] S. Frigoli, C. Fuganti, L. Malpezzi, S. Serra, *Org. Process Res. Dev.* **2005**, *9*, 646.
- [11] A. O. King, N. Yasuda, *Top. Organometal. Chem.* **2004**, *6*, 205.
- [12] L. Yin, J. Liebscher, *Chem. Rev.* **2007**, *107*, 133.
- [13] R. F. Heck, J. P. Nolley, *J. Org. Chem.* **1972**, *37*, 2320.
- [14] T. Mizoroki, K. Mori, A. Ozaki, *Bull. Chem. Soc. Jpn.* **1971**, *44*, 581.
- [15] A. F. Littke, G. C. Fu, *Angew. Chem. Int. Ed. Engl.* **2002**, *41*, 4176.
- [16] A. T. Myller, J. J. Karhe, T. T. Pakkanen, *Appl. Surf. Sci.* **2010**, *257*, 1616.
- [17] A. K. Ferreira, R. Meneguel, A. Pereira, O. M. R. Filho, G. O. Chierice, D. A. Maria, *Anticancer Res* **2012**, *32*, 95.
- [18] M. Zarghani, B. Akhlaghinia, *Appl. Organometal. Chem.* **2015**, *29*, 683.
- [19] M. Zarghani, B. Akhlaghinia, *RSC Adv.* **2015**, *5*, 87769.
- [20] S. Sayin, F. Ozcan, M. Yilmaz, *Mater. Sci. Eng. C* **2013**, *33*, 2433.
- [21] a) T. Azadbakht, M. A. Zolfigol, R. Azadbakht, V. Khakizadeh, D. Perrin, *New J. Chem.* **2015**, *39*, 439; b) M. A. Zolfigol, T. Azadbakht, V. Khakizadeh, R. Nejatyami, D. Perrin, *RSC Adv.* **2014**, *4*, 40036; c) M. A. Zolfigol, V. Khakizadeh, A. R. Moosavi-Zare, A. Rostami, A. Zare, N. Iranpoor, M. H. Beyzavie, R. Luque, *Green Chem.* **2013**, *15*, 2132; d) N. Koukabi, E. Kolvari, A. Khazaei, M. A. Zolfigol, B. Shirmardi-Shaghasemi, H. R. Khavasi, *Chem. Commun.* **2011**, *47*, 9230; e) M. A. Zolfigol, M. Yarie, *RSC Adv.* **2015**, *5*, 103617; f) M. Safaiee, M. A. Zolfigol, F. Afsharnadery, S. Baghery, *RSC Adv.* **2015**, *5*, 102340.
- [22] S. Qu, H. Yang, D. Ren, S. Kan, G. Zou, D. Li, M. Li, *J. Colloid Interface Sci.* **1999**, *215*, 190.

## Supporting Information

Additional supporting information may be found in the online version of this article at the publisher's web site.